

**DEPARTMENT OF THE INTERIOR  
U.S. GEOLOGICAL SURVEY**

**U.S. Geological Survey Committee for the Advancement of  
Science in the Yucca Mountain Project Symposium on "Fractures,  
Hydrology, and Yucca Mountain": Abstracts and Summary**

**by**

**Joan Gomberg<sup>1</sup>, editor**

**Open-File Report 91-125**

This report is preliminary and has not been reviewed for conformity with U.S. Geological Survey editorial standards or with the North American Stratigraphic Code. Any use of trade, product, or firm names is for descriptive purposes and does not imply endorsement by the U.S. Government.

<sup>1</sup>USGS, MS 966  
Box 25046  
Denver Federal Center  
Denver, Colorado 80225

**1991**

**U.S. Geological Survey Committee  
for the Advancement of Science in  
the Yucca Mountain Project**

**Symposium on**

**"Fractures, Hydrology, and Yucca  
Mountain":**

**Abstracts and Summary**

**September 13 & 14, 1990  
Denver, Colorado**

## Table of Contents

	Page
Statement of Objectives by Devin Galloway .....	1
Summary of Talks, Posters, Discussions, and Outstanding Issues by Joan Gomberg .....	2
Symposium Agenda .....	6
List of Posters .....	8
Abstracts:	
<i>Fractal Scaling of Fracture Networks in Rock</i> by Christopher Barton .....	9
<i>Some General Properties of Joints and Joint Networks in Horizontally Layered Sedimentary and Volcanic Rocks -- An Overview</i> by Earl Verbeek and Marilyn Grout .....	10
<i>Seismic Imaging for Fracture Characterization and Structural Definition</i> by E.L. Majer, J.E. Peterson, L.R. Myer, T.M. Daley, K. Karasaki, and T. V. McEvelly .....	13
<i>Regional-scale Velocity Anisotropy Inferred from Nevada Test Site Nuclear Test P-arrivals</i> by Stephen Harmsen .....	14
<i>Fracture Counts from Borehole Logs</i> by P.H. Nelson, R. Snyder, and J.E. Kibler .....	15
<i>Fracture Studies in the Welded Grouse Canyon Tuff: Laser Drift of the G-Tunnel Underground Facility, Rainier Mesa, Nevada Test Site, Nevada</i> by S.F. Diehl, M.P. Chornack, H.S. Swolfs, and J.K. Odum .....	16
<i>Distribution of Fracture-lining Minerals at Yucca Mountain</i> by B. Carlos, D. Bish, S. Chipera .....	18
<i>Stress Field at Yucca Mountain and in Surrounding Regions</i> by Joann Stock .....	20
<i>Field Description and Measurement of Mesoscopic Faults with Application to Kinematic and Paleostress Analyses</i> by Scott Minor .....	21
<i>Rhyolite Flow Fields as Barriers to Paleohydrologic Flow in Eastern Nevada and Western Utah Between Latitudes 37°30'N and 30°N</i> by R. Ernest Anderson and Theodore Barnhard .....	23
<i>Saturated-Zone Ground-Water Flow at Yucca Mountain, Nevada: Can Fracture Flow Be Adequately Characterized?</i> by J. Czarniecki and A. Geldon .....	25
<i>Modeling of Flow and Transport in Fracture Networks</i> by K. Karasaki, A. Davey, J. Peterson, K. Hestir, and J. Long .....	27

<i>Fluid Flow in Rough-Walled Fractures</i> by Robert Zimmerman, Sunil Kumar, and Gudmundur Bodvarsson .....	28
<i>Modeling of Flow and Solute Transport through a Variable Aperture Partially Saturated Fracture</i> by Richard Healy and Edward Kwicklis .....	29
<i>Flow Through Variable Aperture Fractures</i> by John Smoot .....	31
<i>Void Structure and Flow in Single Fractures</i> by Larry Myer .....	32
List of Attendees .....	34

# Statement of Objectives

by

**Devin Galloway**

**U.S. Geological Survey  
2800 Cottage Way, Rm W2239  
Sacramento, CA 95825  
916-978-4648**

## Statement of Symposium Objectives

The principal objective of this symposium is to review the available information on fractured/faulted terrains in terms of a coherent hydrogeologic model of ground-water fluid flow and transport, particularly as it pertains to the Yucca Mountain region. This review addresses the influence and significance of fractures on ground-water flow and the transport of conservative-species solutes within the context of the hydrogeologic setting of the Yucca Mountain area. The relations between fluid flow and fractured or faulted host rock are examined integrally from information on geologic, seismologic, hydrologic, and geomechanical properties of the system. The development of new hydrogeologic approaches that incorporate information from this integrated database are contrasted with more standard approaches toward understanding flow in fractured reservoirs.

Ground-water flow in both the unsaturated zone and the saturated zone are considered. The application of various models of flow is addressed; examples include porous-media equivalent and discontinuum fracture-network models. Data and interpretations from the Yucca Mountain area are presented to establish a context for information exchange. The symposium includes discussions relevant to technical considerations for characterizing the Yucca Mountain area hydrogeology. On the basis of these discussions, CASY has compiled this document in order to formally summarize the proceedings and communicate recommendations for future directions of research and investigation.

**Summary of Talks, Posters, Discussions, Outstanding Issues**

by  
Joan Gomberg

Branch of Geologic Risk Assessment  
US Geological Survey  
Box 25046, MS 966  
Denver Federal Center  
Denver, Colorado 80225  
303-236-4410

This introduction summarizes the information presented at the symposium and some of the outstanding gaps in our understanding of the relationship between fractures and the hydrologic system. Fractures refer to adjacent surfaces in a rock where brittle failure has occurred. When there is only shear motion on a fracture it may be called a fault, and often the term fault also implies that the fracture has length of the order of a km or more. Joints typically refer to fractures with no shear and possibly normal motion across the failure surface. The symposium was appropriately opened with the challenging proposal that the nature of the problem at hand is such that it will never be possible to predict details of future hydrologic systems (Neuzil talk). Rather, it may only be possible to define an envelope of possibilities. If this is the case, the shape and size of such an envelope is as yet unknown so that further studies are required to determine if this view is in fact justified and whether such an envelope is sufficiently small to be useful. Alternatively, a somewhat less bleak view is that we are acquiring knowledge at a rate too slow to be able to adequately address the hydrologic issues facing us at Yucca Mountain but that there is no fundamental limitation to what we can learn. If this is the case, or if one views the potential for scientific progress more positively, then continued investigations must be pursued. In other words, whatever one's views of the state of the science are, further study is essential.

In contrast to the lack of consensus on the state of the science, there was near unanimity among participants that progress to date has been far too slow. This sentiment was expressed by symposium participants in the wrap-up session and in informal discussions. This slow progress is evidenced by the lack of recent work presented by the Yucca Mountain Project (YMP) participants and the dearth of new data from the vicinity of Yucca Mountain. The lively scientific debate inspired throughout the symposium

strongly suggests that significant scientific progress will be made only when data collection in the field is restored.

Fracture descriptions have yielded some important insights into their generation and evolution. The application of fractal theory to fractures (Barton abstract) demonstrates that fractures follow fractal scaling laws over many orders of magnitude in length; this suggests that a single physical process may govern all fracture phenomena. Another implication of fracture generation being governed by a fractal process is that one fracture influences another. Thus, it is important to study a set of fractures collectively and to conduct studies of fractures with scales ranging from microfractures to faults. A statistical study of joint characteristics (Verbeek and Grout abstract) also has demonstrated that a systematic approach to the description of fractures can yield an understanding of their generation (e.g. lithologic control, effects of temporal and spatial sequence in a suite of fractures). Although some work is being done (Minor abstract), much lesser emphasis has been placed on systematically and quantitatively describing characteristics of faults.

It is now possible to make direct observations of fractures at shallow depths (less than a few kilometers). Borehole logs from Yucca Mountain indicate that the relationship between fracture count (derived from television logs) and flow (as inferred from resistivity logs) is not simple (Nelson et al. abstract). Hydraulic tests in boreholes coupled with fracture data from televiwer logs from the same holes also indicate a complex relationship between degree of welding, fracture distribution and interconnectedness and ground water flow direction, magnitude, and travel time (Czarnecki and Geldon abstract). In addition to serving as windows to view fractures in situ, the use of boreholes provides core samples to examine the fine details of fractures ( Carlos et al. and Diehl et al. abstracts). Mineralization in microfractures can serve as keys to paleo flow patterns. Microfractures observed in core samples from the unsaturated zone (Grouse Canyon tuff) are often lined and sealed shut with hydrous mineral phases (Diehl et al. abstract). In situ stress measurements also have been made in the holes left from the core sampling providing estimates of the present state of stress. The stress variations can be interpreted as arising from lithologic differences (e.g. welded vs non-welded tuffs) and are consistent with the abundance and orientation of fractures. Thus, one might conclude that the paleo stress conditions were similar to the present stress conditions, that they are/were conducive to the opening of microfractures, and that the hydrologic conditions were quite different in the past such that water flowed through the fractures resulting in significant mineralization within the microfractures.

Detailed analyses of the distribution of various minerals lining microfractures observed in cores from and very near Yucca Mountain provide evidence of a horizontal stratigraphic control on the paleo flow system. The mineral types and their sequencing serve as clues to the evolution of past water chemistry and thus, possible paleo flow paths and hydrologic conditions. Many of the minerals appear unaltered, suggesting that little water has flowed through the fractures since the last episode of mineralization occurred. However, the observations also suggest that microfractures have undergone reactivation and therefore it is possible that they might operate as viable future transport paths (Carlos abstract) should the climatic conditions change. Attempts to determine the age of mineralization must be made to fully define paleo flow patterns, and further petrographic analyses must be conducted to better define the lateral extent and abundance of mineralization. Apparently many valuable core samples exist but are not available for analysis, thereby making it nearly impossible to properly address these key issues.

Less direct observations of fractures are now being made using seismic methods (vertical seismic profiling, cross-hole tomography, local earthquake/explosion travel time delay analyses). These are proving to be viable tools for mapping fracture distributions on useful vertical scales (e.g., of a single stratigraphic unit such as Paintbrush Tuff at NTS; Majer et al. abstract) and horizontal scales (e.g., to resolve variations between Yucca Mountain and Crater Flat; Harmsen abstract). However, because the methods are indirect and thus interpretation of results is inherently non-unique application of such methods must be combined with other independent types of studies.

The generation of fractures is dependent on the local and regional stress field and on the pre-conditioning of the rocks (e.g., existing fractures, rheologic properties). In situ stress measurements from Yucca Mountain show that stresses are close to those necessary for failure of optimally oriented normal faults and that there is a dynamic relationship between the stress conditions and the water table level (Stock abstract). The opening of fractures may serve as new conduits for flow causing a rise in the water table. Conversely, a rise in the water table due to climatic changes may result in opening of fractures thereby resulting in a tectonically induced change in the water table. Fault control on the paleo-hydrologic system is evidenced in the Eccles basin in eastern Nevada and in the Hamlin Valley of western Utah (Anderson and Barnhard abstract). In both areas faults appear to have acted as the major pipelines to the surface for transport of carbonate-rich water from in a deeply circulating regional ground water system. The strong relationship between

water table, stress conditions, and/or faulting is also made evident by the changes observed in the hydrologic system following the Loma Prieta earthquake (Rojstaczer talk). However, the physics governing this interaction are not understood (Rudnicki talk) and the distribution and characteristics of seismogenic faults are not well known.

The tremendous importance of fractures as controls on hydrologic flow seems to be an accepted scientific premise (Czarnecki and Geldon abstract). The advent of fast computers makes it possible to construct complex models of flow through a single fracture (Healy and Kwicklis, Smoot, and Myer, abstracts) or through a more complex system of fractures (Zimmerman et al., Karasaki et al. abstracts; Kelkar, Czarnecki talks). In order for these complex models to be useful as predictive tools, there must be an adequate amount of data to constrain them. The major source of uncertainty in modeling studies now seems to arise from a lack of adequate data rather than a poor understanding of the fundamental physics and/or numerical techniques (Karasaki et al. abstract). It is now an appropriate time to make serious efforts to coordinate modeling studies with data gathering activities. We now have models of flow in the Yucca Mountain region (Czarnecki talk). If these models are to be made useful, we must focus our efforts on timely gathering and analyses of the relevant data and on the free exchange and innovative use of scientific information.

## Symposium Agenda

September 13, 1990

Time

7:45-8:15

**Registration**

8:15-8:30

**Announcements**

8:30-9:00

**I. Overview -**

"The role of fractures in groundwater hydrology", C. Neuzil (USGS-R)

**II. Fracture Generation & Behavior**

A. Descriptive tools

9:00-9:30

1. Fractals -

"Fractal analysis of fracture networks", C. Barton (USGS-D)

9:30-10:00

2. Statistics -

"Statistical properties of real fracture networks", E. Verbeek (USGS-D)

10:00-10:15

**Coffee Break**

B. Observational constraints

10:15-10:45

1. Field-

"Field description and measurement of mesoscopic faults with special application to kinematic and paleostress analyses", S. Minor (USGS-D)

10:45-11:15

2. Fracture mineralization -

"Distribution of fracture-lining minerals at Yucca Mtn", B. Carlos (LANL)

11:15-11:45

3. Seismic anisotropy-

"Seismic imaging for fracture characterization and crustal definition", E. Majer (LBL)

11:45-1:00

**Lunch**

C. Models

1:30-2:00

"Void structure and flow in single fractures", Larry Myer (LBL)

2:00-2:15

**Coffee Break**

**III. Stress & Strain as Driving Functions for Flow**

A. Regional Stress/strain field

2:15-2:45

"The stress field at Yucca Mountain and in surrounding regions", J. Stock - (Harvard)

2:45-6:30

**YMP Posters/Refreshments/Informal Discussion**

**September 14, 1990**

- 8:15-8:30      **Recap of Previous Day**, R. Wheeler (USGS-D)
- 8:30-9:00      "Hydrologic information squeezed from the response of pore fluids to crustal deformation", S. Rojstaczer (Duke)
- 9:00-9:30      **B. Earthquakes**  
                  "Earthquakes and fluid flow", J. Rudnicki (Northwestern)
- IV. Flow Models**
- A. Modeling**
- 9:30-10:00      "Modeling flow and solute transport through a variable aperture, partially saturated fracture", R. Healy (USGS-D)
- 10:00-10:15    **Coffee Break**
- 10:15-10:45    "Modeling of flow in fracture networks", K. Karasaki (LBL)
- 10:45-11:15    "Computer modeling of 3-D coupled heat-mass-stress effects", S. Kelkar (LANL)
- 11:15-11:45    "Flow through variable aperture fractures", J. Smoot (PNWL)
- 11:45-1:00     **Lunch**
- B. Applications to Yucca Mountain**
- 1:30-2:00      "Modeling saturated-zone ground-water flow at Yucca Mountain and vicinity: can we adequately simulate fracture flow?", J. Czarnecki (USGS-D)
- 2:00-2:30      "Application of discrete fracture analysis to repository characterization and performance assessment", Tom Doe (Golder Assoc.)
- 2:30-2:45      **Coffee Break**
- 2:45-4:00      **Wrap-Up -** K. Karasaki (LBL), D. Galloway (USGS-S), D. Gillies (USGS-D)

Abbreviations:    USGS-D = USGS Denver,      USGS-M = USGS Menlo Park,  
                          USGS-R = USGS Reston,      PNWL = Pacific NW Lab,  
                          LANL - Los Alamos National Lab,  
                          LBL - Lawrence Berkley Lab,    USGS-S = USGS Sacramento

## Posters

"GSIS and Fractures at Yucca Mountain"  
Downey, Kolm, Turner, and Ervin.

"Rhyolite flow fields as barriers to paleohydrologic flow in eastern Nevada and western Utah at latitude 37°30'N"  
E. Anderson, T. Barnhard

"Rock-water interaction in ash-flow tuffs, Yucca Mountain, Nevada: The record from uranium studies"  
R. Zielinski

"Fracture influence on seismic velocities, Rainier Mesa to Yucca Mountain"  
S. Harmsen

"Determining fracture system geometry from well tests"  
T. Doe

"Hydrologic analysis of periodic strain waves: atmospheric, Earth tide, and seismic"  
D. Galloway

"Fracture studies in the Welded Grouse Canyon Tuff: Laser drift of the G-Tunnel underground facility, Rainier Mesa, Nevada Test Site, Nevada"  
S. Diehl, M. Chornack, H. Swolfs, J. Odum

"Fracture counts from borehole logs"  
P. Nelson, R. Snyder, J. Kibler

"Structure of the upper crust (0-4 km) at Yucca Mountain"  
W. Mooney

"Flow in rough-walled fractures"  
Zimmerman, Kumar, Bodvarsson

"Mapping the base of the Tertiary with seismic reflection profiles in Crater Flat and Yucca Mountain"  
T. Brocher

## Fractal Scaling of Fracture Networks in Rock

Christopher C. Barton (U.S. Geological Survey, Box 25046, MS 913, Federal Center, Denver, CO 80225)

The mathematical construct of fractal geometry is well suited to quantify and model spatial and size-scaling relations within complex systems that are statistically self-similar over a broad range of scales. My results show that natural fracture networks in rock follow a fractal scaling law for fractures ranging in length over ten orders of magnitude, from microfractures in tectonically deformed quartz and plagioclase grains to transform faults in the South Atlantic sea floor. Detailed measurements of two-dimensional samples of three-dimensional fracture networks in rocks of dissimilar age, lithology, and tectonic settings show fractal dimensions in the range 1.6-1.8. The small range in fractal dimension implies that a single physical process of rock fracturing operates over this wide range of scale, from microscopic cracks to large, intra-plate fault systems.

Field evidence has established that rock fracturing is an iterative process in which preexisting fractures influence the formation of subsequent fractures (such behavior is characteristic of fractal processes). Fracture networks are not random but evolve from initially ordered to increasingly disordered patterns, and they become more complex with time as new fracture generations are added to those that already exist. The spatial distribution of fractures within the network evolves as fractures are sequentially added to the network. The fractal dimension, which is a quantitative measure of the spatial distribution of the fracture traces, ranges from about 1.33 in early stages of network development to 1.80 for mature networks. The fractal dimension of each successive fracture generation is less than that of the preceding generation, but the fractal dimension for the cumulative network increases as each new generation is added. The fractal behavior implies that fracture-network development is governed by a nonlinear equation. Fortunately, the ability of fractal mathematics to accurately quantify and model the spatial and size-scaling properties of the system is not dependent on specific knowledge of this equation.

# SOME GENERAL PROPERTIES OF JOINTS AND JOINT NETWORKS IN HORIZONTALLY LAYERED SEDIMENTARY AND VOLCANIC ROCKS-- AN OVERVIEW

Earl R. Verbeek and Marilyn A. Grout

The past fifteen years have seen an unprecedented surge in the study of joints, spurred largely by the need to understand the fluid-flow properties of natural fracture systems both to ensure the safe storage of toxic and radioactive wastes and to more effectively recover gas and oil from fractured reservoirs. Joints no longer are the enigmatic features they once were; it is now realized that their properties are related to lithology and to stratal sequence in consistent and understandable ways. The following discussion summarizes some general properties of joints and joint networks and is based on recent work in diverse geologic settings of horizontal to gently tilted sedimentary and volcanic rocks.

## **Orientations**

Strike dispersions of  $15^{\circ}$ - $30^{\circ}$  within individual sets are common; barring complications, the data often approximate normal distributions. Smaller dispersions, as little as  $5^{\circ}$ , have been documented for some early-formed sets within fine-grained, well-cemented, brittle rocks. Strike dispersions tend to increase with increasing thickness of the jointed layer, with increasing grain size, and especially with decreasing degree of induration. The greatest dispersions result from jointing of lithologically heterogeneous units (e.g., a variably cemented channel sandstone) over protracted spans of time during which regional stresses progressively change in orientation; dispersions of  $60^{\circ}$ - $70^{\circ}$  have been documented but are uncommon. In such cases, too, strike-frequency distributions for individual sets can be decidedly non-normal. Within any given jointed layer, strike dispersions of the earliest set tend to be least and of succeeding sets progressively greater.

Dips of joints within thin, planar-bedded, well-cemented rocks commonly are within a few degrees of vertical. As with strikes, dip dispersions tend to increase with increasing thickness and grain size of the jointed layer and with decreasing degree of induration; dip dispersions of  $20^{\circ}$ - $30^{\circ}$ , and locally more, within thick (>3m), weakly cemented sandstones are not uncommon. The influence of bedding on joint dip is seen in the many places where the dip dispersion for a given set is less than the corresponding strike dispersion.

## **Dimensions**

Heights of joints are influenced primarily by the thickness of the individual depositional units in a stratigraphic sequence and by the degree of lithologic contrast between them. Small joints are characteristic of thinly bedded sequences of contrasting rock type (e.g., limestone or chert layers alternating with shales), whereas the opposite is true for thick, internally homogeneous units (e.g., massive sandstones and the massive upper parts of some ash-flow sheets) and within sequences characterized by low lithologic contrast (e.g., some lacustrine siltstones). Far more common, however, are jointed stratal sequences characterized by variable bed thickness and moderate lithologic contrast between beds; common examples include stacked sequences of point-bar sandstones and siltstones. Joints in such deposits show a predictably wide range in height, from small joints confined to individual siltstone partings to large joints that cut several beds in succession; ranges of two to three orders of magnitude are common.

A rough correspondence between joint height and length is often observed, though few exposures offer sufficient three-dimensional control to quantify the relation. Joint lengths for early-formed joints likely are related to magnitude of driving stress, but for later sets the influence of pre-existing joints becomes increasingly important. Joint lengths for successive sets will tend to be progressively shorter if older joints remain open so that younger joints terminate against them, but no such relation need exist where older joints are healed and younger joints cut across them unimpeded. Here again, as in unfractured rock, driving stress may play a major role in influencing joint length. Examples are known where younger joints are longer on average than those formed earlier.

Frequency distributions of joint length for mesoscopic joints often follow a power-law distribution; i.e., progressively shorter joints are present in increasingly greater abundance than longer ones. The claim of a continuum of the power-law relation to microscopic joints has not, to our knowledge, been demonstrated for any area; most workers, for practical reasons, have imposed an arbitrary lower bound on the lengths of the fractures they measured and thus have left undocumented the most critical part of the distribution. Field observations in several areas have shown that small joints, those with trace lengths of several centimeters or less, are present in lesser numbers than are larger joints of the same set, suggesting that the actual frequency distribution of joint lengths may not be a power-law function for short joints.

### Spacings

Spacings of joints are influenced primarily by the lithology and thickness of the jointed layer. For any given lithology a strong relation between mean (or median) joint spacing and layer thickness at the outcrop scale often is evident. The functional form of the relation has been debated, but review of older work supplemented by much new work suggests that equations of the form  $\log S = m \log T + c$ , where  $S$  = median joint spacing,  $T$  = layer thickness, and  $m$  and  $c$  are constants dependent on lithology, hold for the entire range of  $S$  and  $T$  so far examined.  $S$  vs.  $T$  values for different joint sets in the same exposure plot as parallel but generally noncoincident lines that express quantitatively the greater abundance of one set relative to another for any given layer thickness. For different rock types the  $S$  vs.  $T$  values generally plot as lines of different slope; hence, the abundance of joints in one rock type relative to their abundance in another is itself a function of layer thickness.

The above relations hold only where the boundaries between jointed layers are well defined and the individual joints span the full thickness of the layer. Where instead the lithologies are gradational from one layer to another, as among layers defined by different degrees and combinations of welding and devitrification within an ash-flow sheet, the joints, like the rocks, show gradually changing properties vertically. Mechanical contrasts within ash-flow sheets tend to be most pronounced in the lower portions of the sheet, where large differences in degrees of welding and devitrification occur over short vertical distances, and tend to be more obscure within the thick, massive, partially welded to nonwelded tuff that forms the upper parts of some sheets. Complications also arise within layers whose thicknesses are much greater than the heights of individual fractures. The joints in some such rocks, particularly massive sandstones, tend to congregate within zones. Each zone contains multiple, overlapping, closely spaced, and commonly interconnected joints separated by broader intervals of less-fractured rock. Zonal

development of joints has been little studied and is incompletely understood.

### **Interconnections**

Joints can terminate either by dying out within the rock, commonly as tapering cracks decreasing gradually to zero aperture, or by abutting pre-existing fractures. In addition, younger fractures can intersect older ones. The relative proportions of "blind" endings, terminations, and intersections commonly are variable from set to set and are a function of the age of a set relative to others in the same rock, the mineralization history of pre-existing sets, and to some degree the spacings of fractures already present. For obvious reasons blind endings are common and intersections rare among members of the earliest joint set, but abutting relations can also be formed in abundance as later-formed members of a set "hook" into earlier ones to form so-called J terminations. Hence, fluid flow through interconnected fractures can be effective in a rock even if only one set of joints is present. Joints of later sets will tend to abut earlier ones if these are open but intersect them if they have been "healed" effectively by mineralization. Variable proportions of abutting and crosscutting relations are common where early joints are incompletely mineralized and lenticular vugs remain, or where the mechanical contrast between mineral fill and wall rock is sufficient to stop the propagation of some joints but not of others. In any case, the degree of interconnection between younger and older joints tends to be very high unless the older joints are unusually sparse and thus widely spaced within the rock. Poorly to moderately interconnected joint networks, in our experience, are rare.

### **Surface shape**

Early joints in many areas of relatively thick and homogeneous rock have roughly elliptical surfaces with their long axes parallel to bedding. As layer thickness decreases and progressively more joints span the full thickness of the layer, the joints progressively approach a more rectangular form, with flat top and bottom edges. Joint surfaces in thinly bedded sequences of high lithologic contrast tend to be long and ribbonlike, quite unlike their counterparts in thicker layers.

Joint surfaces of later sets exhibit a wide range in form dependent on layer thickness, abundance of fractures already present, and the degree to which these earlier fractures interfered with the propagation of the newer fractures through the rock. In relatively thick layers already cut by abundant joints it is common for the vertical dimensions of later joints to exceed the horizontal.

### **Cross-sectional shape**

From field observations it is apparent that many early-formed joints in relatively homogeneous rock have a maximum wall separation near their midpoints and gradually taper to zero width at either end. Cross-sectional shape as a function of joint size has been little studied, but for one area we have shown that wall separations at joint midpoints are linearly related to joint heights (in a vertical cut) over the total height range of 1-360 cm. Joint shape in this area, then, is relatively constant regardless of joint size, and the largest joints possess by far the largest apertures.

No such relation seems to exist for joints of later sets. Instead, where late joints terminate at both ends against open, pre-existing fractures (free surfaces), the wall separations of the later fractures may be roughly constant along their length, in sharp contrast to early-formed joints in the same rock.

## Seismic Imaging for Fracture Characterization and Structural Definition

*E. L. Majer, J. E. Peterson, L. R. Myer, T. M. Daley  
K. Karasaki, and T. V. McEvilly*

*Center for Computational Seismology, Lawrence Berkeley Laboratory,  
Berkeley, California 94720*

VSP and crosshole tomographic methods are being developed and tested as part of DOE's nuclear waste program for characterizing the Yucca Mountain site. Work has been progressing in the development of models for understanding seismic wave propagation in fractured 3-d heterogeneous media and in field testing fracture characterization methods. These field experiments have been utilizing high frequency (1000 to 10000 Hz.) signals in a cross-hole configuration at scales of several tens of meters. Three component sources and receivers are used to map fracture density, and orientation. The goal of the experiments has been to relate the seismological parameters to the hydrological parameters, if possible, in order to provide a more accurate description of a starting model for hydrological characterization. Results of these controlled experiments indicate that the fractures have a significant effect on the propagation of the P and S-waves. Laboratory experiments indicate that saturation also has a dramatic effect as well. Work involving the verification of the stiffness theory indicates that the theory is valid and at high frequencies (greater than a few kilohertz) the greatest effect is on the amplitude, and at lower frequencies the greatest effect is on the velocity or delay of the seismic waves. In addition to these controlled experiments, multicomponent VSP work has been carried out at several sites to determine fracture characteristics. The results to date indicate that both P-wave and S-wave can be used to map the location of fractures. In addition, fractures that are open and conductive are much more visible to seismic waves than non-conductive fractures. Recent work at the Nevada Test Site indicates that the Paintbrush Tuff is heterogeneous with respect to both P- and S-wave properties. There is observed anisotropy in the shear wave VSP data, but the anisotropy seems to be associated with near surface sediments (100 meters and less) and not associated with the Tuff.

The southern Great Basin seismic network (SGBSN) stations (mostly vertical component or two components), which span an approximately circular region of radius 160 km, centered on Yucca Mountain, show strong azimuthal variation of P-wave travel time delays for Nevada Test Site (NTS) nuclear device tests at Pahute Mesa, Rainier Mesa, and Yucca Flat. Here, delay is defined as observed travel time minus theoretical time, computed from a horizontally isotropic velocity model. For all Yucca Flat, Rainier Mesa, and Area 19 Pahute Mesa tests, the fastest directions, corresponding to the minimum delays, are about north  $10^\circ - 20^\circ$  east and south  $10^\circ - 20^\circ$  west. The slowest directions (maximum delays) appear to be approximately perpendicular to this orientation. One-second variations of travel-time delay with azimuth are observed for Rainier Mesa sources, for paths having lengths less than 100 km. Figure 1 shows the azimuthal distribution of SGBSN station delays for the Rainier Mesa test "Disko Elm" as open circles (all Rainier Mesa nuclear test delay patterns are very similar). The function values,  $a \cos^2(\theta - 10^\circ) + b$ , where  $\theta$  = source to station azimuth, shown as solid triangles for comparison with observed delays (correlation coefficient,  $\rho = 0.8$ ), are, to first order, theoretical delays for P-waves sampling a locally azimuthally anisotropic crust.

Because local earthquake travel time residuals have not been observed to display  $180^\circ$  periodicity, and the delays from the NTS tests do not increase with distance beyond about 70 km, it is likely that sources (structures, stresses, subparallel cracks and microfractures, or intrinsic anisotropy) responsible for the nuclear test travel time anomalies are at shallow depths. The regional direction of minimum horizontal stress, inferred from earthquake focal mechanisms and in agreement with results from Rainier Mesa stress measurements and from shallow hydrofrac determinations at Yucca Mountain, approximately coincides with the low-velocity direction, suggesting that contemporary stresses may be contributing an azimuthal imprint to acoustic velocities, possibly according to the extensive-dilatancy anisotropy model.

Crustal heterogeneity probably plays a larger role than fracture-induced seismic anisotropy in determining the observed delays. Rock at shallow depth ( $< 5$  km) in the Silent Canyon caldera has lower velocity than surrounding country rock, explaining in part the travel-time retardation from Yucca Flat and Rainier Mesa to northwestern SGBSN stations, although no such caldera is present to the east of NTS to explain the eastward delay. Examination of contour plots of SGBSN station delays indicates that many travel-time anomalies are geographically fixed, independent of the nuclear-device test source region, suggesting that local structures rather than regional stresses are the primary sources of the travel-time anomalies. Where SGBSN coverage is densest, around Yucca Mountain (six stations), local variations are visible in velocity, for example, a structural discontinuity between Crater Flat and Yucca Mountain. Carbonate rocks at shallow depths, such as dolomite, have been determined to have greater velocity than clastic rocks at shallow depths at NTS. High-velocity travel-time contours trend roughly parallel to the CP thrust, which exposes many carbonate rocks. Thus, apparent anisotropy in P-wave velocity may be attributed in part to shallow stress orientation relative to discontinuities (fractures and faults), lithologic differences at shallow depth (carbonates versus clastics), or both. The regional network travel-time delays may therefore provide useful information on the distribution and orientation of aquifers and aquitards, in the absence of other anomalies.

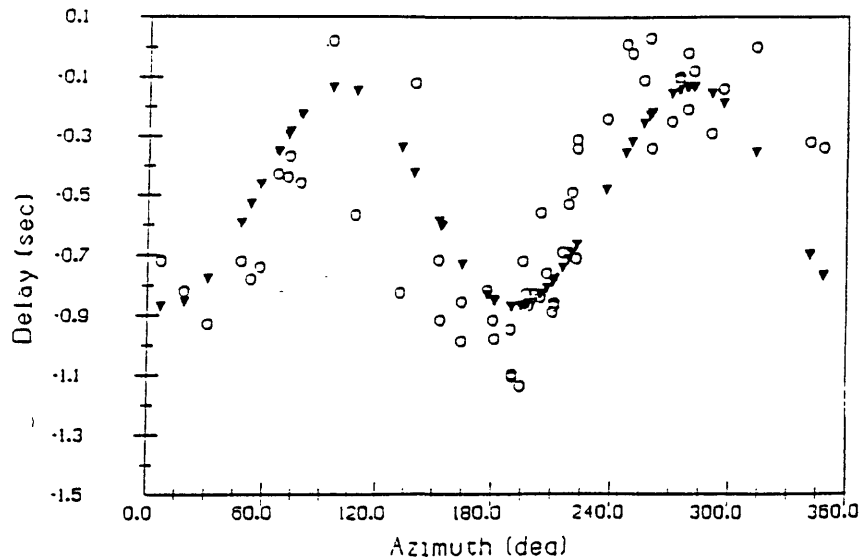


Figure 1. -- Azimuthal distribution of SGBSN station delays for the Rainier Mesa test "Disko Elm." Open circles indicate observed delays; solid triangles indicate function values.

## Fracture Counts from Borehole Logs

by P. H. Nelson, R. Snyder, and J. E. Kibler  
U. S. Geological Survey, Denver

Fractures detected by the sonic waveform, televiewer, and television tools in borehole H-4 at Yucca Mountain are plotted as a function of depth alongside caliper, density, resistivity, and flow logs. Of the three fracture logs, the sonic waveform log provides the least information on individual fractures because spatial resolution is lower and the fracture count is less than that recorded by the televiewer or television tools. The televiewer provides a lower fracture count than the television tool and almost all fractures detected by the televiewer are also recorded by the television tool. The televiewer shows that most fractures dip steeply and have a median dip angle of 79 degrees (dip angle could not be obtained from the television tool). The azimuth of the dip vector is roughly WNW. If a dip-measuring capability could be added to the television tool, then it would be the preferred tool for recording fractures because more fractures are recorded with it than with the televiewer and because it operates in both liquid-filled and air-filled boreholes (the televiewer requires a liquid-filled borehole). However, the television tool's image may be obscured if the borehole liquid contains excessive amounts of suspended solids.

The flow log from the H-4 borehole shows that the most permeable zones lie in the upper parts of the Bullfrog and Tram Members of the Crater Flat Tuff. The television log shows that these two zones are among the most fractured zones in the lower 650 m of the H-4 borehole. Resistivity and density logs indicate that neither zone is altered (zeolitic). Based on information from cored boreholes at Yucca Mountain, the low resistivity zones are interpreted to be zeolitic with minor smectite: in general, they are zones of no flow or low flow with few or no fractures. The lower part of the Tram Member is a good example of a low resistivity, no-flow unit with few fractures.

The flow log was divided into 37 intervals and the change in percent flow vs. fracture count from television was plotted. The plot shows a number of zones with fractures but no flow, one zone with flow but no fractures, and a scatter of data that shows no obvious increase of flow with increased fracture count. However, when cumulative flow vs. cumulative fracture count is plotted, then a monotonic step-wise curve demonstrates that flow does, in general, increase with fracture count. In this borehole, there are no prominent single-fracture "thief zones" contributing most of the flow nor are there zones of intense fracturing contributing most of the flow.

Fracture Studies in the Welded Grouse Canyon Tuff:  
Laser Drift of the G-Tunnel Underground Facility, Rainier Mesa,  
Nevada Test Site, Nevada

By S.F. Diehl, M.P. Chormack, H.S. Swolfs, and J.K. Odum

We studied fractures in the welded Grouse Canyon tuff in the Laser Drift of the G-Tunnel Underground Facility (GTUF) located in Rainier Mesa, about 64 km northwest of Mercury, Nevada. The Grouse Canyon Tuff has lithologic properties, stress conditions, and an overburden depth comparable to those of the proposed repository horizon at Yucca Mountain.

Several horizontal boreholes were cored in the Laser Drift as part of the Yucca Mountain prototype testing program. The USGS conducted surveys in these boreholes using a borehole video camera and video tape recorder. Video tapes of the boreholes were used to detect the presence and orientation of fractures intersecting the boreholes. The numbers of fractures observed in the video surveys compare well with fracture counts during the examination and logging of the recovered core samples from the boreholes. The video tape recording did offer the advantage of a more accurate count of fractures in rubble zones, which were impossible to reconstruct from the core once it had been removed from the borehole.

The boreholes were oriented to intersect the prominent fracture trends (N. 25° E. and N. 40° E.) exposed in the Laser Drift. Most of the fractures are relatively planar with near-vertical dips. Mineralization along the fractures generally consists of iron and manganese staining, but one predominant fracture, trending N. 5° E. with a dip of 86° SE, is filled with clay.

Four microfracture trends that average N. 75° W; N. 29° W; N. 3° E; and N. 70° E. were determined from two oriented samples. Microfracture orientations commonly are perpendicular and parallel to welding and are abundant around stress-concentration points of phenocrysts. Authigenic mineral phases commonly seal microfractures, which indicates precipitation of these minerals from fluids moving through the microfractures. Adularia and iron, titanium, manganese, and rare earth mineral phases fill the microfractures. A few adularia-filled microfractures are parallel to and at 45° to the plane of welding.

The microfractures appear to be extensional in origin. A profile of shut-in pressures from hydraulic fracture testing in two vertical holes near the GULF site (Warpinski and others, 1981) indicates that the least horizontal stress magnitude in the welded Grouse Canyon is half as much as in the adjacent nonwelded units. Thus, the welded unit is in a state of extension, probably due to lateral spreading in the more ductile nonwelded tuff.

Although the Grouse Canyon tuff is currently in the unsaturated zone, the hydrous mineral phases that coat fracture surfaces and seal microfractures indicate that fluid movement has occurred along these structures. This shows that the microfractures were once well-connected flow paths for fluid movement.

Warpinski, N.R., Northrop, D.A., Schmidt, R.A., Vollendorf, W.C., and

Finley, S.J., 1981, The formation interface fracturing experiment—an in situ investigation of hydraulic fracture behavior near a material property interface: Sandia National Laboratories Report SAND81-0938, 82 p.

Distribution of Fracture-lining minerals at Yucca Mountain  
B. Carlos, D. Bish, S. Chipera

Fracture-lining minerals in the tuffs at Yucca Mountain, Nevada are being examined as part of an ongoing study to characterize potential flow paths away from the proposed repository horizon. To date, only an incomplete knowledge of the lateral variability in fracture mineralogy has been obtained because of the limited number of existing cored holes and incomplete sampling of most of these cores. Portions of the Topopah Spring Member have been examined from USW G-2 (north of the proposed repository block), USW G-1, USW GU-3 (south of the proposed repository block), UE25a#1 (east of the block), and water well J-13 (in Jackass Flat). Only the core from USW G-4 has been examined over its entire depth, and fracture coatings in that core appear to be related to stratigraphic interval.

#### Tiva Canyon Member

Most fractures in the Tiva Canyon Member of the Paintbrush Tuff have partial coatings of manganese oxide dendrites (10-60% coverage) and fine grained white powder or crusts of palygorskite with minor mordenite and opal CT (5-40% coverage). Rancieite is the only manganese oxide mineral identified so far, but other minerals such as lithiophorite or todorokite may be present. Many other fractures contain the silica minerals tridymite, cristobalite, and/or quartz coating 75-100% of the fracture surface. The manganese oxide dendrites and fine-grained white silicates are generally on top of the silica minerals when they occur in the same fracture.

#### Topopah Spring Member

Fracture coatings in the devitrified interior of the Topopah Spring Member of the Paintbrush Tuff can be divided into three groups. The first group consists of the lithophysal fractures formed during devitrification of the tuff and formation of the lithophysal cavities, which they often connect. Like lithophysae, the fractures have bleached altered zones surrounding them and coatings of tridymite, or cristobalite or quartz pseudomorphs of tridymite. Although the fracture surfaces are now 100% coated and many are sealed, later deposition of calcite and other minerals demonstrates that some flow paths remained open after the initial formation of these fractures. The calcite commonly fills the lower part of the lithophysal cavities. Zeolites occur with or without calcite in lithophysal cavities and brecciated lithophysal fractures in the lower lithophysal zone in USW G-2, and euhedral quartz occurs with or without fluorite over lithophysal coatings in USW G-3.

The second group of fracture coatings consists of smooth, nearly planar fractures with partial coatings of manganese dendrites and fine-grained mordenite. Lithiophorite is the only manganese oxide identified to date, but scanning electron microscope examination suggests rancieite and/or todorokite may be present in some samples. These fractures crosscut lithophysal fractures, but are believed to be early, possibly cooling fractures. Slickensides have developed on many of these fractures.

The third group includes all later, generally coarse-grained, fracture coatings. Later coatings may occur in re-activated earlier fractures or on rougher later fractures. There is extreme variability in mineralogy and distribution of these coatings across Yucca Mountain. The fracture-lining minerals are generally visibly euhedral, and the fractures are not slickensided. Coatings include heulandite, stellerite, and mordenite in USW G-2 and USW G-1, rosettes of smectite clay in USW G-1, heulandite and mordenite in USW G-4 and UE25a#1, and drusy quartz in J-13 and USW GU-3. In GU-3, fluorite occurs with some of the quartz. Fractures may be partially sealed or open and probably have channels resulting from irregularities in the coatings.

Fracture coatings in the basal vitrophyre of the Topopah Spring Member are fine-grained white to beige with manganese dendrites and appear similar in all cores, but the

mineralogy varies laterally and with depth. Fracture coatings cover 100% of the fracture surface and slickensides are common. Smectite, heulandite and manganese oxides predominate, but erionite has been identified from single samples in USW GU-3, USW G-4, and UE25a#1. Phillipsite occurs in UE25a#1 a meter below the erionite. The presence of different minerals in close proximity suggests localized conditions and limited flow within the vitrophyre.

Fractures in the non-welded Topopah Spring Member below the vitrophyre from USW G-4 and USW G-2 contain a druse of clinoptilolite, sometimes overlying the cristobalite. This interval has not been examined in other cores.

#### Tuff of Calico Hills

Few fractures occur in the tuff of Calico Hills in USW G-4. Fracture coatings are predominantly mordenite and clinoptilolite, covering 80-100% of the fracture surface. Because of the fibrous nature of the mordenite, fractures may be more permeable than the rock matrix even if the fractures are closed.

#### Crater Flat Tuff

There is a close relationship between matrix and fracture mineralogy throughout most of the Crater Flat Tuff in USW G-4. Zeolites are similar to those seen in the tuff of Calico Hills and occur primarily in fractures in zeolitic tuff. Coatings cover 100% of the fracture surface. A few fractures in zeolitic tuff contain manganese oxides and hematite, which tend to be diffused into the matrix.

Devitrified intervals have a few corroded lithophysal fractures. Manganese oxide coatings are common in the devitrified intervals, with or without quartz or calcite. Quartz and calcite-filled fractures are often sealed. The manganese oxide minerals are mostly pyrolusite and cryptomelane-hollandite. In the Tram Member, manganese oxide minerals are intergrown with spherulites in the matrix adjacent to the fractures. Fracture surface coverage is 100% in almost all fractures. Hematite occurs with manganese oxides in many fractures in the lowest part of the Tram.

Below the water table, pump tests provide more information on hydrology than fracture mineralogy does. More than 75% of the water produced from USW G-4 came from the interval in the Tram Member containing abundant manganese oxides and hematite on fractures. As the water producing intervals are different in other holes, and the core from those intervals has not been examined, it is not known whether manganese oxides are generally abundant in water producing intervals in the Crater Flat Tuff.

Joann M. Stock

USGS, MS 977, 345 Middlefield Road, Menlo Park CA 94025; also at Dept. Earth & Planetary Sciences, Harvard Univ., 20 Oxford St., Cambridge MA 02138

The stress field in southern Nevada is constrained from observations of earthquake focal mechanisms, hydraulic fracturing stress measurements, borehole breakouts, and drilling-induced hydraulic fractures<sup>1,2</sup>. Focal mechanisms indicate normal faulting on NE-striking planes, and strike-slip faulting on variably oriented planes, suggesting a combined strike-slip and normal faulting stress regime at seismogenic depths (5-15 km), with the least principal stress,  $\sigma_3$ , approximately horizontal and oriented NW-SE to E-W. Because both strike-slip and normal faulting mechanisms are observed, the maximum and intermediate principal stresses,  $\sigma_1$  and  $\sigma_2$ , respectively, may be close in magnitude to one another. Hydrofrac tests at Rainier Mesa and borehole breakouts in drill holes at Yucca Flat and Pahute Mesa give  $S_h$  (least horizontal principal stress) directions of N45°W-N55°W and N45°W-N60°W, respectively<sup>3,4</sup>.

Magnitudes of stresses within the saturated zone at Yucca Mountain were determined from hydraulic fracturing tests in four wells (USW-G1, USW-G2, USW-G3, and Ue25-p1). In 12 tests from 650-1700 m depth, "new" hydraulic fractures were created to determine the magnitude of  $S_h$ . In all cases, the vertical stress,  $S_v$ , exceeded both the measured value of  $S_h$  and estimates of the maximum horizontal principal stress,  $S_H$ . These measurements indicate a normal faulting stress regime, with values of  $\phi = (\sigma_2 - \sigma_3) / (\sigma_1 - \sigma_3)$  ranging from 0.25 to 0.7. The observed values of  $S_h$  are close to values at which frictional sliding might be expected to take place on optimally oriented preexisting faults, suggesting that the stress regime may be near failure by extensional faulting. Drilling-induced hydraulic fractures in three of the wells, and borehole breakouts in two of the wells, indicated an  $S_h$  direction of N60°W to N65°W, in agreement with other stress field indicators.

Three hydraulic fracturing measurements were attempted in the unsaturated zone in USW-G2, but these tests all appeared to have reopened preexisting fractures and hence only place upper bounds on the value of  $\sigma_3$ . An elastic model assuming lateral restraint has been used to predict the magnitudes and orientations of the principal stresses in the unsaturated zone<sup>5</sup>, but these have not been confirmed by actual measurement.

The water level in the holes at Yucca Mountain ranged from 385 m to 752 m below the surface. Measured values of  $S_h$  were less than surface hydrostatic pressure (the pressure of a column of water reaching the surface in the drill hole). Under these circumstances, favorably oriented water-filled fractures might propagate if the fluid pressure were to increase. This may have happened during drilling in three of these holes, as circulation of drilling fluid could not be maintained back to the surface and large volumes of drilling fluid were lost at depth. Long vertical fractures visible on the borehole televiewer logs from these holes are interpreted to be hydraulic fractures formed during drilling. These drilling induced hydraulic fractures, in conjunction with the low  $S_h$  magnitudes, are important because they suggest a dynamic balance between the magnitude of  $S_h$  and the height of the water table. Thus, a substantial rise in the water table in the future might lead to the opening of pre-existing fractures, or the propagation of new hydraulic fractures, thereby drastically affecting the saturated zone hydrology at Yucca Mountain.

- (1) Stock et al., *Jour. Geophys. Res.* v. 90, 8691-8706, 1985.
- (2) Stock and Healy, in *USGS Bulletin 1790*, pp. 87-93, 1988.
- (3) Springer and Thorpe, Rep. UCRL-87018, LLNL, 1981.
- (4) Warren and Smith, *Jour. Geophys. Res.* v. 90, 6829-6839, 1985.
- (5) Swolfs et al., in *USGS Bulletin 1790*, pp. 95-101, 1988.

[for CASY conference, September 13-14, 1990]

FIELD DESCRIPTION AND MEASUREMENT OF MESOSCOPIC FAULTS WITH  
APPLICATION TO KINEMATIC AND PALEOSTRESS ANALYSES

Scott A. Minor  
U.S. Geological Survey,  
P.O. Box 25046, MS 913,  
Denver, CO 80225

As with other types of fractures, faults can have considerable influence on the flow of ground water, acting either as flow conduits or barriers, or both depending on spatial variations in fault characteristics. Physical characterization of faults can be useful to hydrologists in developing realistic ground-water flow models of faulted terranes such as that at Yucca Mountain, Nevada. Perhaps less apparent is the utility of studies addressing the kinematics and causes of faulting, including paleostress determinations. Knowledge of these aspects of faulting in areas of good accessibility can greatly facilitate predictions of fault geometries and internal fault structure in nearby subsurface rock masses lacking adequate structural control. Furthermore, deriving orientations and estimating magnitudes of paleostresses associated with various faulting episodes can be valuable in predicting how the same fractured rocks will respond to the present regional stress field and to local, man-induced stress changes resulting from repository excavation. In the Yucca Mountain region, mesoscopic faults -- faults that commonly can be seen in their entirety in outcrop and that generally show net offsets of  $< 5$  m -- are best exposed and lend themselves well to detailed observation.

Measurable aspects of mesoscopic faults include: 1) orientation; 2) shape (i.e. deviation from planar geometry); 3) surface dimensions; 4) rake of slickenside striae; 5) net offset (or separation); 6) fault-zone width; 7) aperture; and 8) fault spacing. Other important elements of fault zones are composition and structural fabric. Fault zones usually include various combinations and arrangements of fault breccia, clay gouge, and (or) subsidiary fractures, including Riedel shears and tension fractures. Critical in kinematic studies is the determination of slip sense on individual faults using: 1) geometrical relations of various types of subsidiary fractures in and bordering the fault zone, and genetically related to it; 2) asymmetrical polish; 3) tool marks; 4) vesicle smears; 5) arrangement of syn-slip mineral growths; 6) drag folds; and (or) 7) offset features such as marker beds. Important observations concerning the relative age of faults are: 1) presence, type, and spatial distribution of pre-, syn-, and post-slip minerals; 2) cross-cutting relations of faults and slickenside striae; and 3) age constraints from faulted stratigraphic units. Attitudes of bedding, compaction foliations, or other paleodatums and determination of paleomagnetic directions in fault blocks are necessary to test for horizontal- and vertical-axis rotations of faults, respectively.

Fault-slip data, which consist of fault and slickenside-striae orientations and slip-sense determinations from one or more field sites, can be qualitatively characterized using equal-area and rose plots. Fault data subdivided with the aid of these graphical plots can be inverted using established computational methods to find best-fit orientations of the principal stresses ( $\sigma_1$ ,  $\sigma_2$ , and  $\sigma_3$ , where  $\sigma_1 \geq \sigma_2 \geq \sigma_3$ ). The computed ratio  $\phi = (\sigma_2 - \sigma_3) / (\sigma_1 - \sigma_3)$  is indicative of the relative magnitudes of the principal stresses. Extreme values of the ratio, which ranges from 0 to 1, in conjunction with other analytical parameters, indicates that two of the three principal stresses can not be reliably distinguished from each other using the analyzed data subset. A computation-intensive iterative clustering technique can be used to further separate from a mixed-fault data set two or more subsets that are compatible with unique stress solutions and are consistent with known relative-age information. Through this process the faulting and paleostress histories of an area can be more clearly established than is possible through conventional methods.

RHYOLITE FLOW FIELDS AS BARRIERS TO PALEOHYDROLOGIC FLOW IN EASTERN NEVADA AND WESTERN UTAH BETWEEN LATITUDES 37°30' and 38°N.

by R. Ernest Anderson and Theodore P. Barnhard

Spectacularly straight north-flowing drainages with highly symmetrical cross profiles are developed on Miocene basin-fill strata composed of silicic volcanic clasts within a 100 km<sup>2</sup> area, informally known as Eccles basin in easternmost Nevada, and a 12 km<sup>2</sup> area along Wide Hollow west of Enterprise in adjacent westernmost Utah. In Eccles basin, a separate set of slightly less straight northeast-flowing drainages with strongly asymmetric cross profiles are adjacent to and, in part, overlap the north-flowing drainages. A similar set of strongly asymmetric northeast-trending drainages is present in a 200 km<sup>2</sup> area in southernmost Hamlin Valley in western Utah. In all areas, drainages lack the preferred orientation, straightness, or characteristic cross profiles where they traverse adjacent or underlying pre-basin-fill rocks. Those rocks, principally silicic Miocene volcanics, are commonly faulted, tilted, and erosionally beveled beneath the basin-fill strata. In places, the spectacularly straight drainages are developed on erosional remnants of basin-fill strata that only form a thin veneer atop the deformed Miocene volcanics. In contrast to the volcanics, the basin-fill clastic strata are cut by sparse steep mostly north- or northeast-striking faults and are flat lying to gently tilted.

The drainage-pattern development must be controlled by factors, such as contrasts in degree of cementation, that involve large percentages of the basin-fill strata. Although identification of controlling factors is hampered by poor exposures, study of sparse exposures of the basin-fill and lag debris in Eccles basin suggests that the shoulders of the north- and northeast-trending interfluves are underlain by steep drainage-parallel panels within which vein-type carbonate and disseminated carbonate cement is significantly more abundant than intervening parts of the basin-fill strata. Apparently these panels are more resistant to erosion than the uncemented to weakly cemented sediments of the intervening areas which are, accordingly, etched out into straight channelways during the latest cycle of erosion. This lithologic control of drainage-pattern development is, in turn, structurally controlled by sparse map-scale and smaller drainage-parallel steep faults and fractures. The carbonate was introduced from below into the basin-fill strata by circulation in an ancient fracture-controlled

ground-water system. A very high degree of uniformity in physiographic expression in the subject areas suggests uniform average amounts of introduced carbonate such as might be expected in precipitation from a deeply circulating regional ground-water system.

In Eccles basin and Hamlin Valley the conspicuous linear drainage patterns give way northward to normal dendritic patterns in equivalent basin-fill strata. In Eccles basin the boundary between the contrasting drainage patterns is abrupt and trends east-west. The basin-fill strata on both sides of this boundary have a uniform silicic volcanic clast assemblage and appear to have similar average concentrations of carbonate cement. Apparently the chief difference is in the distribution of the cementing material; the distribution of carbonate is uneven and fracture controlled in the topographically high southern parts of the areas and relatively uniform in the lower northern parts. We interpret this difference as a reflection of paleohydrologic conditions related to 1) ponding and rising of shallow elements of a south-flowing regional carbonate aquifer system as it encountered Cenozoic rhyolite flow fields as aquitards, and 2) incomplete mixing of the fracture-controlled rising carbonate waters with shallow local recharge from the siliceous igneous rocks of the Clover and southernmost Indian Peak ranges located south of the areas of basin-fill strata.

Saturated-Zone Ground-Water Flow at Yucca Mountain, Nevada: Can Fracture Flow Be Adequately Characterized?

John B. Czarnecki and Arthur L. Geldon  
Lakewood, Colorado 80225

U.S. Geological Survey,

The hydrology of Yucca Mountain, Nevada, is being characterized by the U.S. Geological Survey to evaluate its suitability as a repository for high-level nuclear waste. Characterization of the saturated-zone flow system of Yucca Mountain and vicinity provides substantial evidence that, at the scale of the repository, fractures have a large effect on ground-water flow. This evidence includes tracejector and temperature surveys in uncased drillholes that show flow occurring in boreholes at fracture locations (determined from acoustic televiewer logs). Additional evidence is indicated from hydraulic-testing results that yield three-component drawdown curves corresponding to release of water from: (1) fractures only; (2) the rock matrix; and (3) both fractures and the rock matrix. Comparison of data from eleven drillholes at Yucca Mountain shows that water-producing intervals occur throughout the Tertiary stratigraphic column, and that no single formation or member produces water in all boreholes. Water-producing intervals apparently occur as a result of the fortuitous intersection of water-bearing joints, shears, and faults, which are not related to the degree of welding or the degree of fracturing. For example, at the C-hole complex, a 1,027 square meter, multi-well site about 2 kilometers southwest of the design repository area, the principal water producing zone in one well was in nonwelded to partially welded tuff; most of the water production in a second well was in moderately to densely welded tuff; and water in a third well was produced subequally from non-welded to partially welded tuff, moderately to densely welded tuff, and tuff breccia. Although south-southeasterly to south-southwesterly trending fractures predominate in the C-holes, no single set of fractures is associated with fluid inflows or production zones identified by temperature logs and tracejector surveys in these wells.

The implications of fracture flow with regard to simulating ground-water movement within the saturated zone are substantial. Models to date have assumed that the flow system could be represented as a porous medium. This was a reasonable assumption because of the large scale (thousands of square kilometers) of the flow system being simulated. Attention now is focussed on a much smaller scale, the distance from the design repository area to the accessible environment (about 5 kilometers). At this scale, careful attention must be paid to fracture occurrence and geometry to assess accurately ground-water flow direction, magnitude, and travel time. Although further hydraulic testing is scheduled at the C-hole complex and elsewhere at Yucca Mountain, it is uncertain (and perhaps unlikely) that hydraulic interconnection from the repository to the accessible environment can be demonstrated, based on the results of previous hydraulic tests of thirty days or less. These tests showed no observable change in water levels in wells greater than 1 kilometer from the pumped well.

# Modeling of Flow and Transport in Fracture Networks

by

*Kenzi Karasaki, Amy Davey, John Peterson,  
Kevin Hestir, and Jane Long*

Field evidence of fracture controlled flow in hard rocks includes a lack of hydrologic connections between boreholes and highly localized and fracture-associated heterogeneous transmissivities in boreholes. Difficulties associated with interpretation of field measurements in such heterogeneous systems and making of model inputs are discussed. The problem of scaling up is one of the most important issues that need to be addressed when constructing a regional scale model using smaller scale measurements. Assuming the flow system as having a fractal nature may prove very useful. Porous medium models and fracture network models are compared and the limitations of both approaches are discussed. The largest difference between the two approaches lies in the input geometry rather than in the fundamental numerical techniques. The importance of the conceptual model and the philosophy in the application of numerical models is emphasized. Recent developments in modeling of flow and transport in fracture systems are introduced. An advection-dispersion code that uses mixed Eulerian-Lagrangian, adaptive gridding technique is outlined. The model minimizes the numerical dispersion even under high Peclet number conditions. An equivalent discontinuum model and new inversion techniques are introduced. The model does not attempt to reproduce every geometrical detail of the real system. Instead, it attempts to reproduce the observed behavior of the fracture system using simplified geometry while preserving the system's inherent discontinuous nature. The inversion method uses an algorithm called simulated annealing which employs a statistical relation to perform a random global search for the fracture network that best describes the system behavior. This search is equivalent to making a simulation of the fracture network, conditioned on hydrologic measurements of the network. By choosing different seeds for the pseudo-random number generator which drives the search, one can also use the method to obtain confidence intervals for prediction of the hydrologic properties of the fracture system. In this way it is possible to quantify the uncertainty in the hydrologic properties of a fracture network. An example use of an iterated function system model, that is applied using the past UE-25c-hole hydraulic test data, is also shown. The model is generated by a set of affine transformations whose coefficients are determined by an optimization technique.

# Fluid Flow in Rough-Walled Fractures

*Robert W. Zimmerman, Sunil Kumar, and Gudmundur S. Bodvarsson*

Earth Sciences Division  
Lawrence Berkeley Laboratory  
University of California  
Berkeley, CA 94720

Yucca Mountain, Nevada, the proposed site of an underground radioactive waste repository, is composed mainly of volcanic tuffs, some of which are highly fractured. The hydraulic conductivities of the fractured formations at Yucca Mountain are controlled to a large extent by the conductivities of the individual fractures. As it is difficult to measure the permeability of a single fracture *in situ*, it would be advantageous to have a method of relating the permeability to more easily measured properties, such as the fracture roughness profile, percentage contact area, etc. We have used various mathematical models of rock fractures to study the effect of these physical parameters on the permeability.

The effect of the roughness of the fracture surface has been studied using a sinusoidal model of the aperture variation. At low Reynolds numbers, flow in such a fracture is governed by the Reynolds equation. We solve this equation exactly for the two cases of flow parallel to and transverse to the sinusoidal variations, and then use the geometric mean of these two values to estimate the overall permeability. We thereby arrive at an expression for the hydraulic aperture in terms of the mean and the standard deviation of the aperture distribution. The results are in close agreement with the numerical values computed by Brown (J. Geophys. Res., 1989) and Patir and Cheng (J. Lub. Tech., 1978). We have verified that the the results are affected only slightly by the addition of additional sinusoidal components to the aperture distribution.

A different model has been used to assess the effect of contact areas on the permeability. In this model, the fracture is considered to consist of two flat, parallel walls, propped open by cylindrical asperities. A Brinkman-type equation, which is a hybrid of the Navier-Stokes and Darcy equations, is used to model flow through the fracture. This equation accounts for the viscous drag along the sides of the asperities, which has been ignored in previous models. A closed-form expression is derived for the permeability in terms of the percentage contact area, and  $h/a$ , the ratio of the aperture to the asperity radius. The results show that for contact areas on the order of 20-30%, the asperities can reduce the permeability by as much as 50% below the parallel-plate value  $h^2/12$ .

Modeling of Flow and Solute Transport through a Variable  
Aperture Partially Saturated Fracture

by

Richard W. Healy and Edward M. Kwicklis

U.S. Geological Survey, Denver, CO

A numerical model has been developed for simulating water and solute movement through a single rock fracture. The fracture is conceptualized as a two-dimensional grid of nodes. Apertures vary from node to node, producing a fracture profile that resembles a waffle iron. Random values for the log-normally distributed and spatially correlated apertures are generated by Monte Carlo simulation, with mean and variance (VAR) specified by the user. The cubic law is used to calculate transmissivity at each node. Hysteresis in the saturation curve is incorporated into the model for partially saturated. Solute transport is simulated by particle tracking. Diffusion is not included in the model, rather the spread of particle travel times is used as a measure of dispersion.

A sensitivity test was conducted with the model to illustrate the influence of VAR on flow and transport properties of a fracture. Test results showed that as VAR was increased, the average flow rate through the fracture decreased while the variance of the flow rate increased. Average travel time of the particles decreased, but the travel-time variance increased. Hysteresis in the saturation curve also increased as VAR was increased. This model should be useful in evaluating

results of laboratory experiments and in building hypothetical data bases that can be used to evaluate alternative approaches to modeling flow and solute transport through fractures.

# Flow Through Variable Aperture Fractures<sup>1</sup>

John L. Smoot  
Pacific Northwest Laboratory  
P.O. Box 999, MS K6-77  
Richland, WA 99352

## ABSTRACT

The role of fractures in unsaturated flow through welded and nonwelded tuffaceous rocks is a fundamental question being addressed for performance assessment activities in the Yucca Mountain Project. As part of the U.S. Department of Energy's (DOE) PACE-90 exercises, a test case was devised to investigate fracture-matrix interactions for a meter-scale block of Topopah Spring welded tuff (TSw). Documentation of flow at small scales will provide input to development of performance assessment techniques which must realistically be geared to larger scales. The PACE-90 problem consists of modeling flow through a vertical fracture in the TSw block with apertures specified to average from 0.1 to 0.5 mm, which are among the larger apertures expected to occur at depth in TSw. Flow through the fractured block was simulated with the PORFLO-3 code for nonhysteretic, one-phase, unsaturated conditions. Results of initial simulation of simple aperture constrictions and expansions indicate that the presence of variable aperture fractures tended to perturb a predominantly downward flow field within several cm of the fracture. A data set generated by laser scan of an actual fracture was used to generate a fully three-dimensional model of the block. Grid-mesh size considerations did not allow for adequate use of the complete detail in the laser scan so the problem was simplified. The results indicate that dry conditions within the fracture induce flow from the matrix into the fracture; pulses of water input to the top of the fracture produce a gradient of flow into the matrix.

---

<sup>1</sup>This work was supported by the U.S. Department of Energy under Contract DE-AC06-76RLO 1830.

## Void Structure and Flow in Single Fractures

*L. R. Myer*

Earth Sciences Division  
Lawrence Berkeley Laboratory  
Berkeley, CA 94720

The development of a successful geologic repository in a fractured rock mass requires an understanding of the fluid flow in the fractures as a function of stress.

Tests conducted on natural fractures have shown that single phase flow decreases much more rapidly with stress than would be predicted by a model representing the fracture as two parallel plates. However, after cycling, mechanical measurements indicate that fracture deformation, at least in some rock types, is largely elastic. To begin to understand this behavior a liquid metal (Wood's metal) injection technique has been developed in order to obtain casts of the void space in a fracture under different normal loads. These measurements show that while large voids remain even at high stress levels, the connections between these voids become more and more tortuous. One approach to modelling single phase flow is to use a stratified percolation model to generate a correlated aperture pattern similar in appearance to the Wood's metal casts. Fracture deformation is modelled as a uniform reduction in all apertures such that all rock deformation is accommodated by a change in void volume. Using a network model, flow is calculated at each stress level. Results show that this approach satisfactorily simulates the observed relationship between aperture change and flow.

As an alternative approach, the areas of contact in a fracture have been modelled by a "carpet" of cones, so that the contact area increases as fracture deformation increases. Assuming fracture deformation is accommodated by a change in void volume, and using an effective conductance to account for increased tortuosity due to the contact area, good

agreement with observed results has been obtained.

Two phase flow and capillary pressure characteristics in a fracture under stress have been simulated using the stratified percolation model. As a zeroth order approximation relative permeability of the non-wetting phase is based on the flow through the critical neck of the pattern, that is, the smallest aperture along the connected path of highest apertures. Flow of the wetting phase is based on flow through the critical connection on one or more percolating paths, and includes a scaling correction to account for tortuosity. Results suggest a critical saturation is needed for two phase flow to exist. In the laboratory, mercury porosimetry measurements have been performed on a single natural fracture to investigate its capillary pressure characteristics as a function of applied stress. In addition, flow measurements have been made using mercury as a non-wetting fluid. Results suggest that relative permeability (of the non-wetting phase) is most sensitive to changes in stress at low stress levels. Comparison with modelling results indicates that the relationships between applied stress and both capillary pressure characteristics and relative permeability are sensitive to the form of aperture distribution.

## Speakers

C. Barton (USGS-D)  
MS 913, Box 25046  
Denver Federal Center  
Denver, CO 80225

B. Carlos (LANL)  
ESS-1, MS D462  
Los Alamos, NM 87545  
FTS 843-6879

J. Czarniecki (USGS-D)  
MS 421, Box 25046  
Denver Federal Center  
Denver, CO 80225

T. Doe (Golder Assoc.)  
4104 148th Ave. NE  
Redmond, WA  
206-883-0777

D. Galloway (USGS-S)  
2800 Cottage Way, Rm 2234  
Sacramento, CA 95825  
916-978-4648

D. Gillies (USGS-D)  
MS 421, Box 25046  
Denver Federal Center  
Denver, CO 80225  
303-236-0546

R. Healy (USGS-D)  
MS 413, Box 25046  
Denver Federal Center  
Denver, CO 80225

K. Karasaki (LBL)  
#1 Cyclotron Rd., Bldg 50F  
Berkeley, CA 94720  
FTS 451-6759

S. Kelkar (LANL)  
MS D443  
Los Alamos, NM 87545  
505-667-4318

E. Majer (LBL)  
Bldg 50E  
Berkeley, CA 94720

S. Minor (USGS-D)  
P.O. Box 25046

Denver Federal Center  
Denver, CO 80225

L. Myer (LBL)  
1 Cyclotron Rd.  
Bldg 50A, Rm 1127  
Berkeley, CA 94720  
415-486-6456

C. Neuzil (USGS-R)  
MS 431  
National Center  
Reston, VA

S. Rojstaczer (Duke)  
Dept. of Geology  
Old Chemistry Bldg.  
Durham, NC 27706  
919-684-5843

J. Rudnicki (Northwestern)  
Dept. of Civil Engineering  
Northwestern University  
Evanston, IL 60208-3109  
708-491-3411

J. Smoot (PNWL)  
PO Box 999  
Richland, WA 99352  
509-376-1352

J. Stock - (Harvard)  
20 Oxford St.  
Cambridge, MA 02138

E. Verbeek (USGS-D)  
MS 913, Box 25046  
Denver Federal Center  
Denver, CO 80225  
303-236-1277

R. Wheeler (USGS-D)  
MS 966, Box 25046  
Denver Federal Center  
Denver, CO 80225  
303-236-1592

### Poster Presenters

E. Anderson (USGS-D)  
MS 966, Box 25046  
Denver Federal Center  
Denver, CO 80225  
303-236-1584

G. Bodvarsson (LBL)

T. Brocher (USGS-M)

415-329-4737

M. Chornack (USGS-D)  
MS 421, Box 25046  
Denver Federal Center  
Denver, CO 80225  
303-236-5180

S. Diehl (USGS-D)  
MS 966, Box 25046  
Denver Federal Center  
Denver, CO 80225  
303-236-1635

T. Doe (Golder Assoc.)  
4104 148th Ave. NE  
Redmond, WA  
206-883-0777

J. Downey (USGS-D)

E. Ervin (USGS-D)  
MS 421, Box 25046  
Denver Federal Center  
Denver, CO 80225

D. Galloway (USGS-S)  
2800 Cottage Way, Rm 2234  
Sacramento, CA 95825  
916-978-4648

S. Harmsen (USGS-D)  
MS 966, Box 25046  
Denver Federal Center  
Denver, CO 80225

J. Kibler (USGS-D)

K. Kolm (USGS-D/CSM)

S. Kumar (LBL)

W. Mooney (USGS-M)

P. Nelson (USGS-D)  
MS 964, Box 25046  
Denver Federal Center  
Denver, CO 80225

J. Odum (USGS-D)  
MS 966, Box 25046  
Denver Federal Center  
Denver, CO 80225

R. Snyder (USGS-D)  
303-236-1263

H. Swolfs (USGS-D)  
MS 966, Box 25046  
Denver Federal Center  
Denver, CO 80225

Turner (USGS-D)

R. Zielinski (USGS-D)  
MS 424, Box 25046  
Denver Federal Center  
Denver, CO 80225  
303-236-4719

R. Zimmerman (LBL)  
MS 50E  
Berkeley, CA 94720  
415-486-7106

## Participants

C. Abrams  
USNRC, ACNW  
MS P-314  
Washington DC 2055  
FTS 492-8371

A. Balch (CSM)

S. Beason (Burec-D)  
Box 25007  
Denver Federal Center  
Denver, CO 80225  
303-236-4177

T. Bjerstedt (DOE-LV)  
US DOE/YMP  
702-794-7590

C. Boughton (USGS-D)  
T. Brady (USGS-D)  
T. Brocher (USGS-M)

C. Boughton (USGS-D)  
303-236-0400

C. Bufe  
Denver Federal Center  
Denver, CO 80225

T. Buono (USGS-LV)  
702-794-7088

F. Byers (USGS-D)  
303-236-5606

W. Carr (USGS,Sandia)  
11345 W. 38th Ave.  
WheatRidge, CO  
303-421-6410

W. Causseau (USGS-D)  
MS 421, Box 25046  
Denver Federal Center  
Denver, CO 80225  
303-236-5307

D. Chesnut (LLNL)  
415-423-5053

M. Ciesnik (USGS-D)  
303-236-1914

J. Coe (USGS-D)  
MS 909  
Denver Federal Center  
Denver, CO 80225  
303-236-0914

J. Cole (USGS-D)  
MS 913, Box 25046  
Denver Federal Center  
Denver, CO 80225

N. Coleman (NRC)  
301-492-0530

C. Cope (USGS-D)  
303-236-5177

P. Covington (SAIC-D)  
303-279-7242

R. Craig (USGS-LV)

J. Devine (USGS-R)

D. Dobson (USDOE-LV)  
702-794-7940

P. Domenico (USNWTRB)  
Arlington, VA

W. Dudley (USGS-D)  
MS 425, Box 25046  
Denver, CO 80225

C. Faunt (CSM/USGS)

C. Fridrich (USDOE-LV)  
702-794-7587

K. Futa (USGS-D)  
MS 963  
Denver Federal Center  
Denver, CO 80225

A. Geldon (USGS-D)  
303-236-0854

J. Gemmell (USGS-D)  
303-236-5014

R. Getzen (USGS-M)  
MS 496  
345 Middlefield Rd.  
Menlo Park, CA

J. Gibbons (ARA)  
4300 San Mateo Blvd.  
Suite A220  
Albuquerque, NM

J. Gomberg (USGS-D)  
MS 966, Box 25046  
Denver Federal Center  
Denver, CO 80225  
303-236-4410

L. Hayes (USGS-D)  
FTS 776-0516

D. Hoxie (USGS-D)  
MS 425  
Denver Federal Center  
Denver, CO 80225  
303-236-5019

P. Justus (USNRC)  
USNRC, MS 4H-3  
Washington DC 20555

K. Kersch (SAIC)  
702-794-7620

L. Kniper (LANL/USGS)  
505-667-1918

J. Krasou (GeoExp. Intl. Inc.)  
5701 E. Evans Ave.  
Denver, CO 80222  
303-759-2746

J. Kume (USGS-D)  
MS 421, Bldg 53  
Denver Federal Center  
Denver, CO 80225  
303-236-5015

E. Kwicklis (USGS-D)  
303-236-6228

R. Laczniak (USGS-LV)  
702-295-0136

G. LeCain (USGS-D)  
303-236-5020

L. Lehman (State of NV)  
612-894-0357

K. Levy (Weston)  
202-646-6779

S. Levy (LANL)  
FTS 843-9504

B. Lewis (USGS-D)

D. Lobmeyer (USGS-D)  
303-236-6227

R. Lucky (USGS-D)  
303-236-5033

F. Maestas (ARA)  
4300 San Mateo Blvd.  
Suite A220  
Albuquerque, NM

S. Mahan (USGS-D)

B. Marshall (USGS-D)  
MS 963  
Denver Federal Center  
Denver, CO 80225

S. Martel (LBL)  
Earth Sciences Division  
415-486-5837

K. McConnell (NRC)  
USNRC, MS 4H-3  
Washington DC 20555  
FTS 492-0532

T. McKee (USGS-M)

M. McKeown (Burec-D)  
303-278-3908

M. Mifflin (State of Nevada)  
2700 Sunset  
Las Vegas, NV 89120

D. Muhs  
MS 424, Box 25046  
Denver Federal Center  
Denver, CO 80225

C. Newberry (USDOE)  
FTS 544-7942

G. O'Brien (USGS-D)  
MS 421, Box 25046

Denver Federal Center  
Denver, CO 80225

G. Patterson (USGS-D)  
303-236-5179

Z. Peterman (USGS-D)  
Bldg. 21B, MS 963  
Denver Federal Center  
Denver, CO 80225  
303-236-7886

C. Peters (USGS-D)  
303-236-0464

D. Plouff (USGS-M)  
345 Middlefield Rd.  
Menlo Park, CA 94025  
415-329-5312

R. Raup (USGS-D)

B. Robinson (LANL)  
MS D443  
Los Alamos, NM 87545  
FTS 843-4318

G. Roseboom (USGS-R)  
703-648-4422

J. Rosenshein (USGS-R)  
414 National Center  
Reston, VA  
703-648-4169

J. Rousseau (USGS-D)  
303-236-5183

C. Savard (USGS-NV)  
Box 327  
Mercury, NV  
FTS 575-5830

S. Schilling (USGS-D)  
MS 913  
Denver Federal Center  
Denver, CO 80225  
303-236-0914

U. Schimschal (USGS-D)

D. Schmidt (USGS-D)  
303-236-1262

M. Schmidt  
303-431-8550

V. Schneider (USGS-R)  
MS 414  
Reston, VA 22092

G. Severson (USGS-D)  
303-236-5032

G. Shideler (USGS-D)  
303-236-1273

R. Shroba (USGS-D)  
MS 913, Box 25046  
Denver Federal Center  
Denver, CO 80225  
303-236-1292

F. Singer (SAIC-D)

R. Spengler (USGS-D)  
MS 913, Box 25046  
Denver Federal Center  
Denver, CO 80225

E. Springer (LANL)  
MS J521  
Los Alamos, NM 87545  
505-667-9836

B. Steinkampf (USGS-D)

G. Stirewalt (NRC)  
CNWRA-NRC  
1235 Jefferson Davis, Suite 1102  
Arlington, VA 22202-3283  
703-979-9129

J. Stuckless (USGS-D)

N. Stuthmann (USGS-D)

E. Taylor (USGS-D)

F. Thamir (USGS-D)  
MS 421, Box 25046  
Denver Federal Center  
Denver, CO 80225

M. Thompson (Sandia)  
505-844-7146

R. Thompson

MS 913  
Denver Federal Center  
Denver, CO 80225

W. Thordarson (USGS-D)  
303-236-5192

C. Throckmorton (USGS-D)  
303-236-1106

V. Tidwell (Sandia)  
505-845-8956

N. Trask (USGS-R)  
FTS 959-5719

S. Wheatcraft (DRI)  
PO Box 60220  
Reno, NV 89512  
702-673-7393

M. Whitfield (USGS-D)

W. Wilson (USGS-D)  
303-922-9107

### **Abbreviations**

USGS-R - USGS Reston  
USGS-D - USGS Denver  
USGS-M - USGS Menlo Park  
USGS-S - USGS Sacramento  
USGS-LV - USGS Las Vegas  
LANL - Los Alamos National Lab  
LBL - Lawrence Berkely Lab  
MIT - Mass. Institute of Technology  
PNWL - Pacific Northwest Lab  
CSM - Colorado School of Mines  
LLNL - Lawrence Livermore Natl Lab  
NRC - Nuclear Regulatory Commission  
USNWTRB - US Nuclear Waste  
Technical Review Board  
Burec-D - Bureau of Reclamation Denver  
DRI - Dessert Research Institute  
SAIC - Science Applications International  
Corp.  
USDOE-LV - US Dept. of Energy, Las  
Vegas